BIOCHEMISTRY
including biophysical chemistry & molecular biology

Article

pubs.acs.org/biochemistry

Evidence for an Unprecedented Histidine Hydroxyl Modification on D2-His336 in Photosystem II of *Thermosynechoccocus vulcanus* and *Thermosynechoccocus elongatus*

Miwa Sugiura,[*,†,‡] Kazumi Koyama,[†] Yasufumi Umena,[‡,§] Keisuke Kawakami,[§] Jian-Ren Shen,[∥] Nobuo Kamiya,[§,⊥] and Alain Boussac[#]

[†]Proteo-Science Research Center, Ehime University, Bunkyo-cho, Matsuyama, Ehime 790-8577, Japan

[‡]PRESTO, Japan Science and Technology Agency (JST), 4-1-8 Honcho, Kawauchi, Saitama 332-0012, Japan

[§]The OUC Advanced Research Institute for Natural Science and Technology (OCARNA), Osaka City University, 3-3-138 Sugimoto, Sumiyoshi, Osaka 558-8585, Japan

[∥]Photosynthesis Research Center, Graduate School of Natural Science and Technology/Faculty of Science, Okayama University, Tsushima-naka, Kita-ku, Okayama 700-8530, Japan

[⊥]Graduate School of Science, Osaka City University, 3-3-138 Sugimoto, Sumiyoshi, Osaka 558-8585, Japan

[#]iBiTec-S, CNRS UMR 8221, CEA Saclay, Gif-sur-Yvette 91191, France

Supporting Information

ABSTRACT: The electron density map of the 3D crystal of Photosystem II from *Thermosynechococcus vulcanus* with a 1.9 Å resolution (PDB: 3ARC) exhibits, in the two monomers in the asymmetric unit cell, an, until now, unidentified and uninterpreted strong difference in electron density centered at a distance of around 1.5 Å from the nitrogen Nδ of the imidazole ring of D2-His336. By MALDI-TOF/MS upon tryptic digestion, it is shown that ∼20−30% of the fragments containing the D2-His336 residue of Photosystem II from both *Thermosynechococcus vulcanus* and *Thermosynechococcus elongatus* bear an extra mass of +16 Da. Such an extra mass likely corresponds to an unprecedented post-translational or chemical hydroxyl modification of histidine.

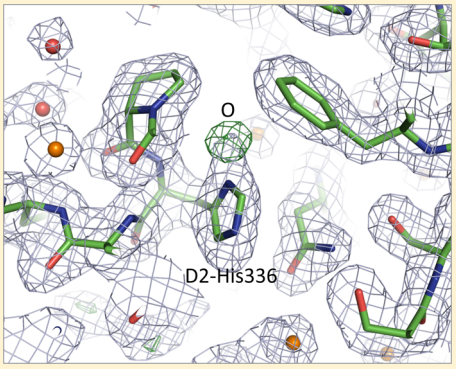

Elucidation of the process of photosynthesis at the molecular level is of paramount importance to contribute to the answer to the problems arising from global environmental changes. Today, engineers and scientists face the challenge of fuels production using sunlight, water, and carbon dioxide. Yet, nature has been performing this reaction for more than 2 billion years using solar energy to remove protons and electrons from water, generate oxygen, trap CO_2, and store the energy in the chemical bonds of biomass (sugars, etc.). Thus, photosynthesis is the ultimate energy input into the biosphere. The light-driven oxidation of water performed by Photosystem II (PSII) is the first step in the entire photosynthetic process.

PSII from cyanobacteria is composed of 17 transmembrane protein subunits and 3 extrinsic proteins[1] (the PsbY unit was missing in ref 1 but is present, for example, in ref 2 and in Sr-containing PSII[3]). Altogether, these bear 35 chlorophylls, two pheophytins, two hemes, one nonheme iron, two plastoquinones (Q_A and Q_B), a Mn_4CaO_5 cluster, two Cl^- ions, 11 carotenoids, and approximately 20 lipids.[1] The excitation resulting from the absorption of a photon is transferred to the photochemical trap that undergoes charge separation. The positive charge is then stabilized on P_{680}, a weakly coupled chlorophyll dimer. Then, $P_{680}^{+\bullet}$ oxidizes Tyr_Z, the Tyr161 residue of the D1 polypeptide, which in turn oxidizes the Mn_4CaO_5 cluster. On the electron-acceptor side, the electron is transferred to the primary quinone electron acceptor, Q_A, and then to Q_B, a two-electron and two-proton acceptor.[2−4] The Mn_4CaO_5 cluster accumulates oxidizing equivalents and acts as the catalytic site for water oxidation. The enzyme cycles sequentially through five redox states, denoted S_n where n stands for the number of stored oxidizing equivalents (n = 0−4). Upon formation of the S_4 state, two molecules of water are rapidly oxidized, resulting in the release of one O_2 molecule and regeneration of the S_0 state,[5,6] see refs 7−10 for recent reviews. The main cofactors involved in stable PSII oxygen evolution activity are borne by two proteins, D1 (PsbA) and D2 (PsbD)

Thermosynechoccocus elongatus, a thermophilic cyanobacterium, has become, over the last 15 years, one of the model organisms used in photosynthesis research for the following reasons. First, the PSII of this organism is very robust, allowing

Received: September 5, 2013
Revised: December 6, 2013
Published: December 9, 2013

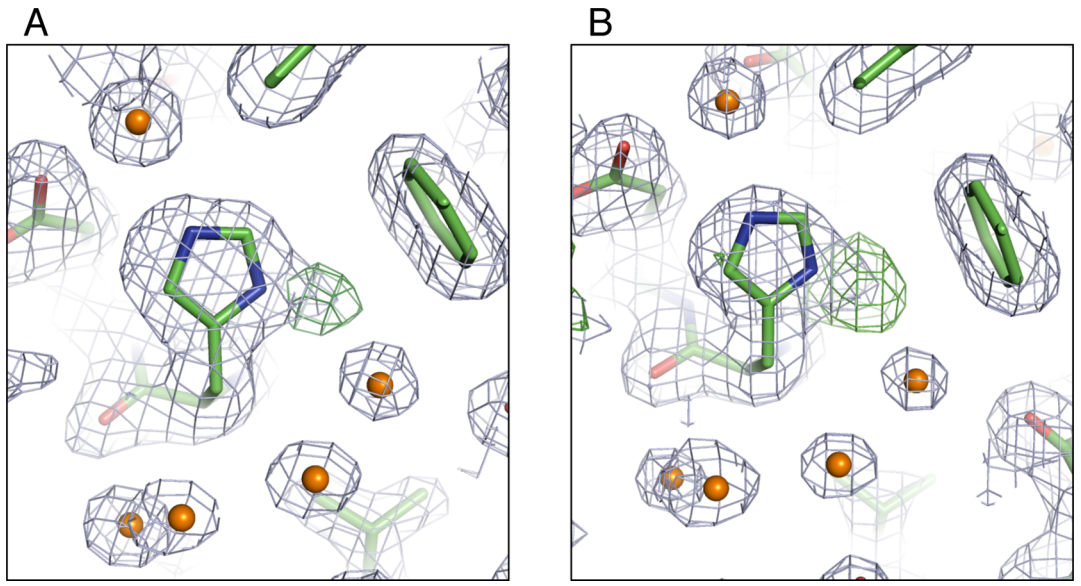

Figure 1. Electron density distributions around D2-His336 of PSII from *T. vulcanus* at 1.9 Å resolution (PDB: 3ARC). (A) Monomer A and (B) monomer B. The distributions depicted in gray are the $2F_o - F_c$ electron densities maps at the 1σ level, and those in green correspond to $F_o - F_c$ difference Fourier maps at the 3σ level. These maps were calculated as an omit electron density map corresponding to the unprecedented modification. The orange balls are water molecules.

enzymological studies with less risks of enzyme denaturation. Second, the first 3D crystallographic structures of PSI and PSII were obtained with enzymes purified from this cyanobacterium.[2,11,12] Third, the genome was sequenced in 2004.[13] Fourth, the molecular biology in this organism is now well-established.[14−24] The structural resolution of 3D crystals obtained with PSII from *T. elongatus* has increased from 3.4 Å[12] to 2.9 Å,[2] and, more recently, the resolution increased to 1.9 Å with a PSII enzyme purified from the very similar cyanobacterium, *Thermosynechococcus vulcanus*.[1]

Analyses of the electron density map calculated from the PSII structure from *T. vulcanus*[1] (PDB: 3ARC) revealed a relatively strong difference in electron density (>3σ) found in the vicinity of some residues. One example is the D1-Tyr246 residue, for which extra electron density possibly originating from an HOO adduct has been suggested.[25] However, it remains to be clarified if an interpretation of this different electron density is relevant to an analysis of the crystal structure at 1.9 Å resolution. Here, we would not address whether the modification is due to functional reasons or is a consequence of radical production during the X-ray exposure. Interestingly, another strong difference in electron density concerns the environment of D2-His336 (Figure 1).

The center of this difference electron density was detected at a distance around 1.5 Å from nitrogen N_δ of the imidazole ring of D2-His336 in both monomers (although it is slightly larger in monomer B). Such an extra electron density could originate from either a post-translational modification or a radical adduct resulting from PSII function or induced by the X-ray beam. In the former case, we wondered if it is specific to *T. vulcanus* or if it is also present in other cyanobacteria, like *T. elongatus*. These two questions are addressed in the present article. The D2 protein was extracted from PSII purified from different *T. elongatus* strains and from *T. vulcanus*. Then, the fragments containing the D2-His336 residue obtained by a trypic digestion were analyzed by MALDI-TOF/MS and LC-MS/MS spectroscopies.

EXPERIMENTAL PROCEDURES

PSII Samples. PSII core complexes from the *T. elongatus* variants WT*1,[18] WT*2,[19] and WT*3,[17] from the *T. elongatus* D2-His189Leu mutant,[16] and from *T. vulcanus* were purified as previously described.[1,16−19]

Mass Spectrometric Measurements. Isolated PSIIs were solubilized with 2% lithium lauryl sulfate and analyzed by SDS-polyacrylamide gel electrophoresis with a 16−22% gradient gel containing 7.5 M urea as described previously.[14,18] All of the buffers used were bubbled with N_2 gas to remove O_2 and therefore to avoid artifactual amino-acid oxidations.[32] The coomassie brilliant blue (CBB)-visualized bands of the protein extracts separated on the SDS gels were subjected to in-gel trypsin digestion as previously reported.[26] Briefly, the gel bands were cut from the SDS gels along their band edges, typically in a size of 1.5 mm wide and 1 mm high (1 mm thick), each gel piece was equilibrated with a solution of 100 mM NH_4HCO_3 (50 mL) for 10 min, and 50 μL of acetonitrile was further added in the tube. The tube was left for 10 min to remove CBB, and the gel piece was washed with water (50 μL) for 10 min followed by dehydration with 20 μL of acetonitrile for 15 min. The solution was discarded, and the gel piece was dried in a vacuum evaporator centrifuge for 20 min. The gel was rehydrated with a solution of 10 mM dithiothreitol in 20 μL of 100 mM NH_4HCO_3 and kept at 56 °C for 1 h. The tube was then cooled to room temperature, and the solution was discarded; twenty microliters of 50 mM iodoacetamide in 100 mM NH_4HCO_3 was added, and the alkylation of cysteine residues was achieved by keeping the tube in the dark for 45 min with mild shaking (room temperature). The gel piece was washed in 50 μL of 100 mM NH_4HCO_3 for 10 min, dehydrated with acetonitrile for 15 min, dried in vacuum, and rehydrated in a 10 μL aliquot of trypsin solution (5 μg mL^{-1} in 50 mM NH_4HCO_3), and trypsin digestion was carried out at 37 °C for 13 h. The solution was placed in a new tube, and the gel was further subjected to peptide extraction with 10 μL of 0.1% trifluoroacetic acid/50% acetonitrile (v/v) for 20 min with

dx.doi.org/10.1021/bi401213m | *Biochemistry* 2013, 52, 9426−9431

sonication. The pooled solution was subjected to vacuum centrifugation until the volume of the solution was reduced to 2 μL. Then, the solution was diluted with 10 μL of water.

Mass spectra of tryptic peptides were acquired with a Voyager-DE PRO MALDI-TOF mass spectrometer (Applied Biosystems) operated in the reflector mode at 20 kV accelerating voltage and 100 ns ion extraction delay, with the nitrogen laser working at 337 nm and 3 Hz in the m/z range of 600−4000 as desribed previously.[20] The tryptic digested peptides were mixed with the same volume of a saturated matrix (sinapic acid, Fluka) solution that consisted of 60% acetonitrile and 0.1% trifluoroacetic acid. Data Explorer software (Applied Biosystems) was used for subsequent data processing and the generation of peak lists.

The fragments with a m/z value close to 2638 and 2654 obtained upon tryptic digestion of the D2 band in the SDS polyacrylamide gel electrophoresis were isolated by reverse-phase chromatography and then further analyzed with LC−MS/MS (analyzed by Genomine, Inc.). Details of this procedure are described in the Supporting Information.

RESULTS AND DISCUSSION

To assign the species responsible of the extra density seen close to D2-His336, the D2 protein band, separated on an SDS-polyacrylamide gel, was digested by trypsin. Then, the resulting fragments were first analyzed by MALDI-TOF mass spectroscopy. Figure 2 shows the MALDI-TOF spectra recorded in the m/z region from 2600 to 2700 in which the peptide fragment of D2 containing the His336 residue is detectable after trypic digestion (i.e., the 327−348 fragment) (see the Supporting Information). Spectrum a corresponds to PSII purified from *T. elongatus* (with PsbA1 as the D1 protein), and spectrum b corresponds to a redissolved crystal sample of PSII from *T. vulcanus*.

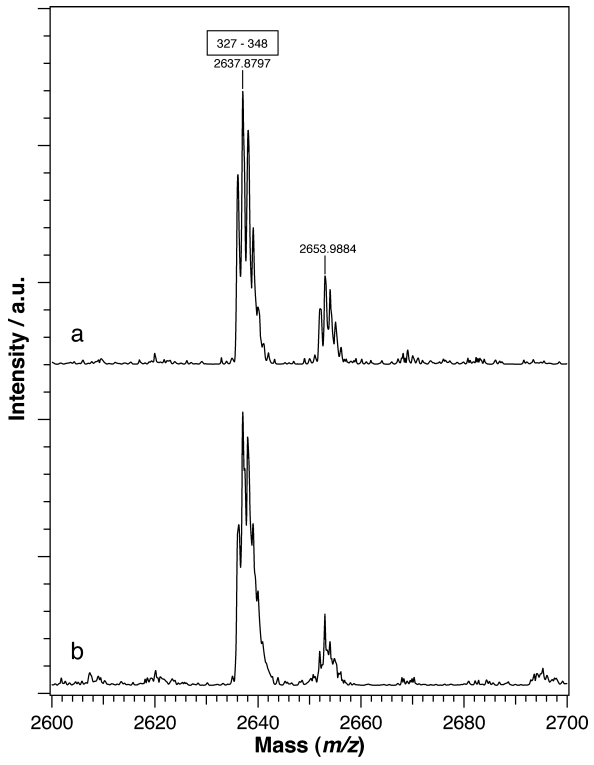

Figure 2. MALDI-TOF mass spectra in reflector mode of isolated PsbA1−PSII complexes from *T. elongatus* in red (spectrum a) and from redissolved crystals of *T. vulcanus* in black (spectrum b). The m/z region shown corresponds to the 327−348 fragment containing the His336 residue obtained upon tryptic digestion of D2. Adrenocorticotropic hormone fragment (m/z 2465.1989 in monoisotopic) and bovine insulin (m/z 5730.6087 in monoisotopic) were used to calibrate the m/z scale.

The two peaks with m/z ∼2638 and ∼2654 were observed in both the *T. vulcanus* and *T. elongatus* samples. The former, which had the larger amplitude, was observed at m/z 2638. This m/z value corresponds to the expected size for a nonmodified 327−348 fragment when no amino acid modification had occurred (Table 1). The second peak, at m/z ∼2654, matches neither the fragments that result from the tryptic digestion of the D2 protein nor two adjacent fragments that would not have been separated by the tryptic digestion (see the Supporting Information). Therefore, it seems very likely that the two different peaks correspond to the same 327−348 fragment, with the presence of an extra mass in the second fragment resulting from certain proportion of PSII. The difference in the m/z value between the two peaks is 16.11. This additional mass is too large for a CH_3 adduct (in this case, the maximum additional mass would be 15.04) and too small for a SH adduct (33.07). Therefore, an oxygen adduct seems to be the most likely possibility. An extra mass of ∼16 can correspond to a hydroxyl addition to the imidazole ring followed by release of a proton.

Table 1. D2 Peptide Fragments Identified by MALDI-TOF Mass Spectroscopy upon Tryptic Digestion in Different PsbA PSII Variants

fragment	n^a	calculated mass^b	experimental mass^c
327−348	22	2636.2482	2653.99 (+17.7)
			2637.88 (+1.63)
234−251	18	2028.9211	2029.23
305−317	13	1546.6828	1547.02
252−264	13	1543.7823	1545.45
13−23	11	1406.6868	1405.52
295−304	10	1256.6037	1258.35

[a]Number of residues in the fragments obtained by tryptic digestion of D2. [b]Average theoretical mass. [c]Experimental mass using the reflector mode.

The fragment exhibiting a m/z value of 2652.14 (i.e., with an extra m/z value equal to +16) was further purified by reverse chromatography (see the Supporting Information) and analyzed with LC−MS/MS (Genomine, Inc.). Then, the 2652 Da fragment was digested by collisions in Ar gas. The new fragments were analyzed by MALDI-TOF, and the full sequence of the original fragment was deduced as being xWMAPxDxPHExFVFPEExLPx, with the extra mass indeed borne by the fragment containing the His336.

To clarify whether the adduct described above depends on the source of PSII preparations, the MALDI-TOF/MS analysis upon tryptic digestion was also performed on (i) a redissolved PSII crystal sample from *T. vulcanus*[1] that was not subjected to X-ray irradiation and (ii) PSII from *T. elongatus* in the presence of either dimethyl sulfoxide or ethylene glycol, two chemicals potentially used in the postcrystallization process for cryo-crystallography. As shown in the Supporting Information, in all of these cases, the same proportion of D2 was found to bear the same adduct.

dx.doi.org/10.1021/bi401213m | *Biochemistry* 2013, 52, 9426−9431

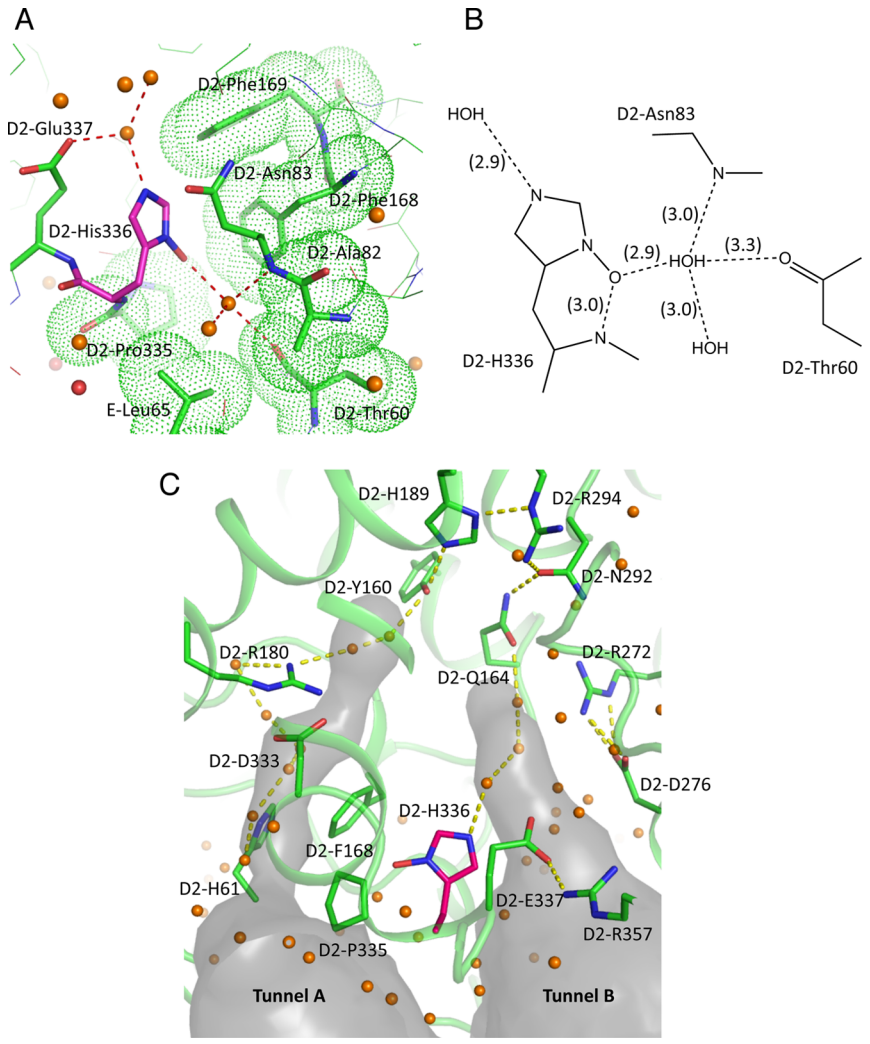

Figure 3. (A) Environment of the proposed hydroxylated D2-His336 based on the 1.9 Å resolution crystal structure. Dot meshes show amino acid residues in van der Waals radii. D2-His336 is surrounded by hydrophobic amino acid residues. The modified hydroxyl group on D2-His336 and the linked water molecule are located in the cavity surrounded by the hydrophobic residues. (B) Hydrogen-bond network. The crystal structure of native PSII (PDB: 3ARC) was further refined, including the hydroxylated D2-His336. Dotted lines and numbers in parentheses show hydrogen bonds and average distances of the two monomers, respectively, in the 1.9 Å resolution crystal structure. Temperature factors corresponding to water molecules, which hydrogen bonded to the hydroxyl group in D2-His336, are both 29 $Å^2$ in monomer A and 34 $Å^2$ in monomer B, respectively; these values are similar to those of amino acid chains surrounding these molecules. The water molecule hydrogen bonded to Nε of D2-His336 is also stable, with temperature factors of 29 $Å^2$ in monomer A and 31 $Å^2$ in monomer B, respectively. (C) Structure of the tunnels connecting to the lumen and involving the hydrogen-bond network and water molecules from Tyr_D, D2-Tyr160, which were calculated with CAVER2.1. The orange balls are water molecules. Tunnel A involves the proton path from Tyr_D to D2-His61 suggested by Saito et al.[31] Here, we propose an additional tunnel, tunnel B, where a proton might be transferred from D2-His189 to D2-His336 through D2-Arg294, D2-Asn292, D2-Gln164, and water molecules. Because D2-His336 is blocking the proton donation by hydrophobic residues D2-Phe168 and D2-Pro335 from tunnel A, tunnel B is separated by D2-His336 from Tunnel A. In tunnel B, D2-Arg357 and D2-Asp276 form salt bridges with D2-Glu337 and D2-Arg272, respectively. These electrostatic interactions might work to maintain the tunnel structure and the linkage structure of the hydrogen-bond network in a stable manner. In contrast, D2-His336 might be the end of the proton network in the absence of its ion-pair partner.

To probe both the accuracy of these measurements further and a possible consequence of the substitution of different *psbA* genes on the proportion of the PSII in which the adduct was observed, different PSII variants that are composed of different D1 subunits, such as PsbA2[19] and PsbA3[17] instead of PsbA1, and a site-directed mutant, D2-His189Leu,[16] were analyzed. In all PSII complexes with the different D1 variants, a peak with m/z 2653 was observed in addition to the peak at m/z 2638 (data not shown). As for the peptide fragment (181−233) containing the D2-His190Leu mutation, it exhibited a m/z value of 5714.91 instead of 5738.80 in the wild type. This decrease in the m/z value by −23.8956 corresponds to the expected decrease for a His to Leu mutation, which demonstrates the accuracy of our measurement.

From the above results, it seems very likely that the extra mass observed from certain proportion of the 327−348 fragment of D2 corresponds to the extra electron density detected in the vicinity of the His336 residue in the 1.9 Å resolution X-ray structural analysis because no other extra electron density was found around the 327−348 fragment of D2. Because the PSII studied in this mass spectroscopic work has never been subjected to X-ray irradiation, this adduct cannot originate from the binding of radicals generated by the X-ray beam. Therefore, the most likely explanation is that the

dx.doi.org/10.1021/bi401213m | *Biochemistry* 2013, 52, 9426−9431

extra mass of m/z 16 corresponds either to a post-translational modification of D2-H336 or to a hydroxylation that would occur in the two thermophilic cyanobacterial species.

Because no EPR signal corresponding to an oxidation of histidine with a $OH^{\bullet}$ is detected in PSII, the occurrence of such an oxidation can be reasonably ruled out. There are some precedences for a peroxide adduct on the Cε atom of the imidazole side chain of histidine, such as 2-oxo-histidine found in the oxidized PerR protein.[27] A hydroxyl adduct on tryptophane has also been found in the lignin peroxidase.[28] However, this hydroxyl adduct is observed either on the C_{β} atom of the tryptophane or on a carbon atom[29] in hydroxyl-radical-mediated modification of proteins. Although an adduct of oxygen to C_{δ} seems possible, a powerful oxidation reaction would be required for this adduct. Therefore, PSII from *T. elongatus* and *T. vulcanus* may have provided the first example of an unprecedented OH adduct on the N atom of the imidazole. As a matter of fact, the addition of the OH group to one of the C atoms of the imidazole side chain of D2-His336 would stabilize the hydrogen-bond network around this amino acid by also involving a water molecule.

As mentioned in earlier, the extra electron density is detectable in both PSII monomers of the dimer in the crystal structure. However, from the amplitude of the peaks at 2637.88 and 2653.99 of the mass-spectra shown in Figure 2, it is clear that the OH adduct was not present in all of the PSII complexes, and we estimate that it is present in 20−30% of the complexes. This contrasts, for example, with the formylation of PsbI in PSII from *T. elongatus*, which was observed in all of the reaction centers.[20] We also performed a short refinement of the structure by restraining the B-factor of the O atom to the average value of the nearby His and water molecule. The result showed that the occupancies of the two O atoms are in the range of 0.5−0.6, which is higher than the 20−30% revealed from the MALDI-TOF analysis. This discrepancy may be caused by several factors. For example, the mass spectra reflects the whole fraction of PSII in solution, whereas the crystal structural analysis is performed with crystals, and it is possible that the modified His residue is preferentially incorporated into the crystals. Alternatively, some of the fraction containing the modified His residue may have escaped the mass detection, probably because of dehydroxylation of the modified His residue by laser illumination or some difficulty in deionization of the specific fragment, resulting in a lower occupancy. In any case, the mass spectra provides a good qualitative analysis that is in agreement with the assignment based on the electron density obtained from the high-resolution structural analysis, but it does not have high accuracy in the quantification of each peak. Because the main purpose of this article is the identification of the electron density seen near D2-His336, we consider that our results have provided enough evidence for the assignment of this extra density.

Further work will be required to identify the functional consequence of this unprecedented histidine modification. It should be noted that D2-His336, although very well conserved, is not present in *Gloeobacter violaceus*. However, the involvement of D2-His336 in the structural stabilization of the hydrogen-bond network in D2 can be proposed. Figure 3A,B shows the distances and possible H-bonds between the modified His336 residue and its environment. As shown in Figure 3B, the modified hydoxyl group of D2-His336 can be hydrogen bonded to the N atom of its own main chain and linked to the N atom of the main chain of D2-Asn83 and O atom of main chain of D2-Thr60 through one of the water molecules. Alternatively, two other functional roles could be suggested. In the first one, the D2-His336 residue would be the end of the proton pathway starting from Tyr_D-His189 in tunnel B, as shown in Figure 3C. In the second one, D2-His336 would act as a hydroxyl-radical scavenger, and the hydroxylated residue observed in the present study could be a result of this scavenging reaction. Some earlier literature has indeed looked at the hydroxylation of PSII subsequent to photodamage.[33] Side-path electron transfers that can be the source of reactive oxygen species production could also potentially lead to the oxidative stress of the PSII complexes, see, for example, ref 30.

■ ASSOCIATED CONTENT

Supporting Information

Amino acid sequence of the D2 protein and digestion sites with trypsin, MALDI-TOF mass spectra in reflector mode of isolated PSII complexes from *T. elongatus* and *T. vulcanus* under various conditions, and D2 peptide fragments identified by MALDI-TOF/MS upon tryptic digestion for different PsbA PSII variants and the D2-His189Leu mutant. This material is available free of charge via the Internet at http://pubs.acs.org.

■ AUTHOR INFORMATION

Corresponding Author

*E-mail: miwa.sugiura@ehime-u.ac.jp. Phone: +81-89-927-9616.

Funding

This work was supported by a grant from the JST-PRESTO program to M.S. (4018).

Notes

The authors declare no competing financial interest.

■ ACKNOWLEDGMENTS

Jérôme Lavergne and Pascal Arnoux are acknowledged for prompting us to do this work. We also thank Professor Keiji Okada (Osaka City University) for helpful discussions.

■ ABBREVIATIONS USED

MALDI-TOF/MS, matrix-assisted laser desorption/ionization time-of-flight mass spectroscopy; P_{680}, chlorophyll dimer acting as the second electron donor; PSI, photosystem I; PSII, photosystem II; Q_A, primary quinone acceptor; Q_B, secondary quinone acceptor; Tyr_D, D2-Tyr160; Tyr_Z, D1-Tyr161; WT*1, WT*2, and WT*3, cells containing only the $psbA_1$, $psbA_2$, $psbA_3$ genes in *Thermosynecococcus elongatus*, respectively

■ REFERENCES

(1) Umena, Y., Kawakami, K., Shen, J.-R., and Kamiya, N. (2011) Crystal structure of oxygen-evolving photosystem II at a resolution of 1.9 Å. *Nature 473*, 55−60.

(2) Guskov, A., Kern, J., Gabdulkhakov, A., Broser, M., Zouni, A., and Saenger, W. (2009) Cyanobacterial photosystem II at 2.9-Å resolution and the role of quinones, lipids, channels, and chloride. *Nat. Struct. Mol. Biol. 16*, 334−342.

(3) Koua, F. H. M., Umena, Y., Kawakami, K., and Shen, J.-R. (2013) Structure of Sr-substituted photosystem II at 2.1 Å resolution and its implications in the mechanism of water oxidation. *Proc. Natl. Acad. Sci. U.S.A. 110*, 3389−3894.

(4) Diner, B. A., and Rappaport, F. (2002) Structure, dynamics, and energetic of the primary photochemistry of photosystem II of oxygenic photosynthesis. *Annu. Rev. Plant Biol. 53*, 551−580.

(5) Kok, B., Forbush, B., and McGloin, M. (1970) Cooperation of charges in photosynthetic O_2 evolution-I. A linear four step mechanism. *Photochem. Photobiol. 11*, 457−475.
(6) Joliot, P., and Kok, B. (1975) Oxygen evolution in photosynthesis, in *Bioenergetics of Photosynthesis* (Govindjee, Ed.) pp 387−412, Academic Press, New York.
(7) Renger, G. (2011) Light induced oxidative water splitting in photosynthesis: Energetics, kinetics and mechanism. *J. Photochem. Photobiol., B 104*, 35−43.
(8) Dau, H., Zaharieva, I., and Haumann, M. (2012) Recent developments in research on water oxidation by photosystem II. *Curr. Opin. Chem. Biol. 16*, 3−10.
(9) Cox, N., and Messinger, J. (2013) Reflections on substrate water and dioxygen formation. *Biochim. Biophys. Acta 1827*, 1020−1030.
(10) Cox, N., Pantazis, D. D., Neese, F., and Lubitz, W. (2013) Biological water oxidation. *Acc. Chem. Res. 46*, 1588−1596.
(11) Jordan, P., Fromme, P., Witt, H. T., Klukas, O., Saenger, W., and Krauss, N. (2001) Three-dimensional structure of cyanobacterial photosystem I at 2.5 angstrom resolution. *Nature 411*, 909−917.
(12) Ferreira, K. N., Iverson, T. M., Maghlaoui, K., Barber, J., and Iwata, S. (2004) Architecture of the photosynthetic oxygen-evolving center. *Science 303*, 1831−1838.
(13) Nakamura, Y., Kaneko, T., Sato, S., Ikeuchi, M., Katoh, H., Sasamoto, S., Watanabe, A., Iriguchi, M., Kawashima, K., Kimura, T., Kishida, Y., Kiyokawa, C., Kohara, M., Matsumoto, M., Matsuno, A., Nakazaki, N., Shimpo, S., Sugimoto, M., Takeuchi, M., Yamada, M., and Tabata, S. (2002) Complete genome structure of the thermophilic cyanobacterium *Thermosynechococcus elongatus* BP-1. *DNA Res. 9*, 123−130.
(14) Sugiura, M., and Inoue, Y. (1999) Highly purified thermo-stable oxygen evolving photosystem II core complex from the thermophilic cyanobacterium *Synechococcus elongatus* having His-tagged CP43. *Plant Cell Physiol. 40*, 1219−123.
(15) Sugiura, M., Rappaport, F., Brettel, K., Noguchi, T., Rutherford, A. W., and Boussac, A. (2004) Site-directed mutagenesis of *Thermosynechococcus elongatus* photosystem II: The O_2 evolving enzyme lacking the redox active tyrosine D. *Biochemistry 43*, 13549−13563.
(16) Un, S., Boussac, A., and Sugiura, M. (2007) Characterization of the tyrosine-Z radical and its environment in the spin-coupled $S_2Tyr_Z^{\bullet}$ state of photosystem II from *Thermosynechococcus elongatus*. *Biochemitry 46*, 3138−3150.
(17) Sugiura, M., Boussac, A., Noguchi, T., and Rappaport, F. (2008) Influence of histidine-198 of the D1 subunit on the properties of the primary electron donor, P_{680}, of photosystem II in *Thermosynechococcus elongatus*. *Biochim. Biophys. Acta 1777*, 331−342.
(18) Ogami, S., Boussac, A., and Sugiura, M. (2012) Deactivation processes in PsbA1-photosystem II and PsbA3-photosystem II under photoinhibitory conditions in the cyanobacterium *Thermosynechococcus elongatus*. *Biochim. Biophys. Acta 1817*, 1322−1330.
(19) Sugiura, M., Ogami, S., Kusumi, M., Un, S., Rappaport, F., and Boussac, A. (2012) Environment of Tyr_Z in photosystem II from *Thermosynechococcus elongatus* in which PsbA2 is the D1 protein. *J. Biol. Chem. 287*, 13336−13347.
(20) Sugiura, M., Iwai, E., Hayashi, H., and Boussac, A. (2010) Differences in the interactions between the subunits of photosystem II dependant on D1 protein variants in the thermophilic cyanobacterium *Thermosynechococcus elongatus*. *J. Biol. Chem. 285*, 30008−30018.
(21) Kawakami, K., Umena, Y., Iwai, M., Kawabata, Y., Ikeuchi, M., Kamiya, N., and Shen, J.-R. (2011) Roles of PsbI and PsbM in photosystem II dimer formation and stability studied by deletion mutagenesis and X-ray crystallography. *Biochim. Biophys. Acta 1807*, 319−325.
(22) Takasaka, K., Iwai, M., Umena, Y., Kawakami, K., Ohmori, Y., Ikeuchi, M., Takahashi, Y., Kamiya, N., and Shen, J.-R. (2010) Structural and functional studies on Ycf12 (Psb30) and PsbZ-deletion mutants from a thermophilic cyanobacterium. *Biochim. Biophys. Acta 1797*, 278−284.
(23) Nowaczyk, M. M., Krause, K., Mieseler, M., Sczibilanski, A., Ikeuchi, M., and Rogner, M. (2010) Deletion of *psbJ* leads to accumulation of Psb27-Psb28 photosystem II complexes in *Thermosynechococcus elongatus*. *Biochim. Biophys. Acta 1817*, 1339−1345.
(24) Iwai, M., Katoh, H., Katayama, M., and Ikeuchi, M. (2004) Improved genetic transformation of the thermophilic cyanobacterium, *Thermosynechococcus elongatus* BP-1. *Plant Cell Physiol. 45*, 171−175.
(25) Saito, K., Rutherford, A. W., and Ishikita, H. (2013) Mechanism of proton-coupled quinone reduction in photosystem II. *Proc. Natl. Acad. Sci. U.S.A. 110*, 954−959.
(26) Manabe, T., and Jin, Y. (2007) Analysis of protein/polypeptide interactions in human plasma using non-denaturing micro-2-DE followed by 3-D SDS-PAGE and MS. *Electrophoresis 28*, 2065−2079.
(27) Traoré, D. A. K., El Ghazouani1, A., Jacquamet, L., Borel, F., Ferrer, J.-L., Lascoux, D., Ravanat, J.-L., Jaquinod, M., Blondin, G., Caux-Thang, C., Duarte, V., and Latour, J.-M. (2009) Structural and functional characterization of 2-oxo-histidine in oxidized PerR protein. *Nat. Chem. Biol. 5*, 53−59.
(28) Choinowski, T., Blodig, W., Winterhalter, K. H., and Piontek, K. (1999) The crystal structure of lignin peroxidase at 1.70 Å resolution reveals a hydroxy group on the C^{β} of tryptophan 171: A novel radicals formed during the redox cycle. *J. Mol. Biol. 286*, 809−827.
(29) Xu, G., and Chance, M. R. (2007) Hydroxyl radical-mediated modification of proteins as probes for structural proteomics. *Chem. Rev. 107*, 3514−3543.
(30) Frankel, L. K., Sallans, L., Limbach, P. A., and Bricker, T. M. (2012) Identification of oxidized amino acid residues in the vicinity of the Mn_4CaO_5 cluster of photosystem II: Implications for the identification of oxygen channels within the photosystem. *Biochemistry 51*, 6371−6377.
(31) Saito, K., Rutherford, A. W., and Ishikita, H. (2013) Mechanism of tyrosine D oxidation in photosystem II. *Proc. Natl. Acad. Sci. U.S.A. 110*, 7690−7695.
(32) Sun, G., and Anderson, V. E. (2004) Prevention of artifactual protein oxidation generated during sodium dodecyl sulfate-gel electrophoresis. *Electrophoresis 25*, 959−965.
(33) Sharma, J., Panico, M., Shipton, C. A., Nilsson, F., Morris, H. R., and Barber, J. (1997) Primary structure characterization of the photosystem II D1 and D2 subunits. *J. Biol. Chem. 272*, 33158−33166.